

Fusion of Probabilistic Projections of Sea-Level Rise

Grandey, Benjamin S.; Dauwels, Justin; Koh, Zhi Yang; Horton, Benjamin P.; Chew, Lock Yue

DOI

[10.1029/2024EF005295](https://doi.org/10.1029/2024EF005295)

Publication date

2024

Document Version

Final published version

Published in

Earth's Future

Citation (APA)

Grandey, B. S., Dauwels, J., Koh, Z. Y., Horton, B. P., & Chew, L. Y. (2024). Fusion of Probabilistic Projections of Sea-Level Rise. *Earth's Future*, 12(12), Article e2024EF005295. <https://doi.org/10.1029/2024EF005295>

Important note

To cite this publication, please use the final published version (if applicable). Please check the document version above.

Copyright

Other than for strictly personal use, it is not permitted to download, forward or distribute the text or part of it, without the consent of the author(s) and/or copyright holder(s), unless the work is under an open content license such as Creative Commons.

Takedown policy

Please contact us and provide details if you believe this document breaches copyrights. We will remove access to the work immediately and investigate your claim.

Earth's Future

RESEARCH ARTICLE

10.1029/2024EF005295

Special Collection:

Regional Sea Level Change and Society

Key Points:

- We fuse the complementary strengths of alternative projections of sea-level rise
- The fusion is a single probabilistic projection that quantifies a best estimate of scientific uncertainty
- The fusion provides a meaningful *very likely* range and an associated high-end projection

Supporting Information:

Supporting Information may be found in the online version of this article.

Correspondence to:

B. S. Grandey,
benjamin.grandey@ntu.edu.sg

Citation:

Grandey, B. S., Dauwels, J., Koh, Z. Y., Horton, B. P., & Chew, L. Y. (2024). Fusion of probabilistic projections of sea-level rise. *Earth's Future*, 12, e2024EF005295. <https://doi.org/10.1029/2024EF005295>

Received 4 SEP 2024

Accepted 15 NOV 2024

Author Contributions:

Conceptualization: Benjamin S. Grandey

Formal analysis: Benjamin S. Grandey

Funding acquisition: Justin Dauwels,

Benjamin P. Horton, Lock Yue Chew

Investigation: Benjamin S. Grandey

Methodology: Benjamin S. Grandey

Project administration: Lock Yue Chew

Software: Benjamin S. Grandey

Supervision: Lock Yue Chew

Validation: Zhi Yang Koh

Visualization: Benjamin S. Grandey




Writing – original draft: Benjamin S. Grandey

S. Grandey

© 2024. The Author(s).

This is an open access article under the terms of the [Creative Commons Attribution License](https://creativecommons.org/licenses/by/4.0/), which permits use, distribution and reproduction in any medium, provided the original work is properly cited.

Fusion of Probabilistic Projections of Sea-Level Rise

Benjamin S. Grandey¹ , Justin Dauwels², Zhi Yang Koh¹, Benjamin P. Horton^{3,4} , and Lock Yue Chew¹ 

¹School of Physical and Mathematical Sciences, Nanyang Technological University, Singapore, Singapore, ²Department of Microelectronics, Faculty of Electrical Engineering, Mathematics, and Computer Science, Delft University of Technology (TU Delft), Delft, The Netherlands, ³Earth Observatory of Singapore, Nanyang Technological University, Singapore, Singapore, ⁴Asian School of the Environment, Nanyang Technological University, Singapore, Singapore

Abstract A probabilistic projection of sea-level rise uses a probability distribution to represent scientific uncertainty. However, alternative probabilistic projections of sea-level rise differ markedly, revealing ambiguity, which poses a challenge to scientific assessment and decision-making. To address the challenge of ambiguity, we propose a new approach to quantify a best estimate of the scientific uncertainty associated with sea-level rise. Our proposed fusion combines the complementary strengths of the ice sheet models and expert elicitations that were used in the Sixth Assessment Report (AR6) of the Intergovernmental Panel on Climate Change (IPCC). Under a low-emissions scenario, the fusion's *very likely* range (5th–95th percentiles) of global mean sea-level rise is 0.3–1.0 m by 2100. Under a high-emissions scenario, the *very likely* range is 0.5–1.9 m. The 95th percentile projection of 1.9 m can inform a high-end storyline, supporting decision-making for activities with low uncertainty tolerance. By quantifying a best estimate of scientific uncertainty, the fusion caters to diverse users.

Plain Language Summary A probabilistic projection of sea-level rise uses a probability distribution to represent uncertainty. Using differing methods, scientists have constructed several alternative probabilistic projections of sea-level rise. By considering their complementary strengths, we propose to combine the alternative projections into a single fusion. The fusion quantifies our best estimate of the uncertainty associated with future sea-level rise. Under a low-emissions scenario, the fusion's *very likely* range of global mean sea-level rise is 0.3–1.0 m by 2100. Under a high-emissions scenario, the *very likely* range is 0.5–1.9 m. The fusion is easy to interpret and caters to diverse users.

1. Introduction

Probabilistic projections of sea-level rise support climate risk assessment and adaptation planning (Hermans et al., 2023; Rasmussen et al., 2020; Rodziejewicz et al., 2022). Each probabilistic projection uses a probability distribution to represent uncertainty (Kopp, Garner, et al., 2023). However, probabilistic projections are undermined by ambiguity (Text S1 in Supporting Information S1; Ellsberg, 1961; Kopp, Oppenheimer, et al., 2023). Much of this ambiguity is due to ice sheet processes (Bamber et al., 2022; Fox-Kemper et al., 2021). Ice sheet models may skillfully represent many important processes, enabling model ensembles to explore the uncertainty associated with these processes (Goelzer et al., 2020; Payne et al., 2021). However, models may fail to represent other important processes (Aschwanden et al., 2021). To complement the models, experts can consider the potential impact of these poorly-understood processes (Bamber et al., 2022). To project sea-level rise, scientists have developed alternative model-based and expert-based methods (Horton et al., 2018). Differing methods drive differences between alternative probabilistic projections (Kopp, Garner, et al., 2023). We refer to this ambiguity as “method ambiguity”.

Method ambiguity poses a challenge to scientific assessment (Kopp, Oppenheimer, et al., 2023). For example, the Sixth Assessment Report (AR6) of the Intergovernmental Panel on Climate Change (IPCC) distinguishes between *medium confidence* and *low confidence* projections (Fox-Kemper et al., 2021). Using the *medium confidence* projections, the AR6 authors derive a *likely* range (17th–83rd percentiles). However, considering the substantial method ambiguity, they note they are unable to derive a *very likely* range (5th–95th percentiles; Fox-Kemper et al., 2021, p. 1298). This poses a challenge to decision-making: the absence of a *very likely* range and the associated 95th percentile high-end projection undermines planning of activities with low uncertainty tolerance.

Writing – review & editing: Benjamin S. Grandey, Justin Dauwels, Zhi Yang Koh, Benjamin P. Horton, Lock Yue Chew

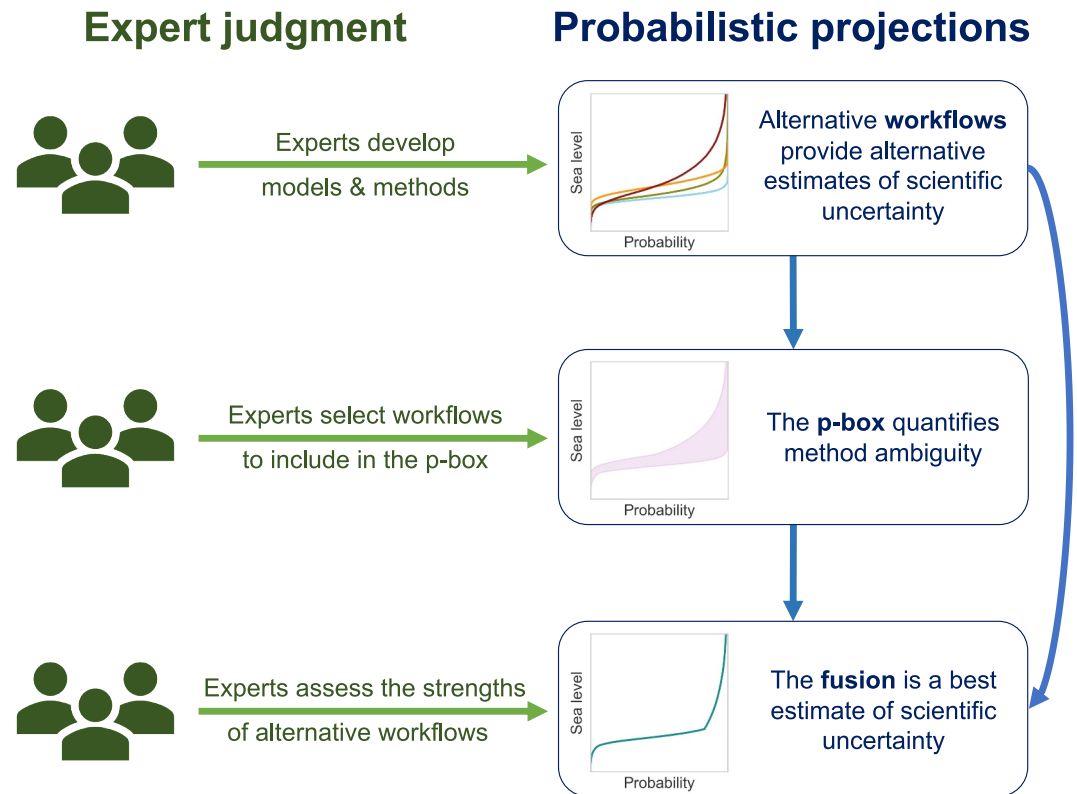


Figure 1. Expert judgment is integral throughout the process of projecting sea-level rise. Arrows indicate the flow of information from expert judgment (green arrows) and from probabilistic projections (blue arrows).

To address the challenge of method ambiguity, we propose a new approach to obtain a best estimate of the scientific uncertainty. We apply an additional layer of expert judgment to combine the complementary strengths of alternative probabilistic projections (Figure 1). We assume that the *medium confidence* projections reliably sample the most-likely central possibilities but underestimate the full range of the uncertainty distribution. We also assume that the *low confidence* projections offer valuable information about less-likely possibilities in the tails of the uncertainty distribution. Our proposed fusion is an informed best estimate of the scientific uncertainty, conditioned on our assumptions and a specific emissions scenario. We apply our fusion approach under both a low-emissions and a high-emissions scenario. Using the fusion, we can derive a *very likely* range and a 95th percentile projection, supporting decision-making.

2. Methods

2.1. IPCC AR6 Projection Workflows

We use data from the IPCC AR6 sea-level projections (Fox-Kemper et al., 2021; G. G. Garner et al., 2021; Kopp, Garner, et al., 2023). The global mean sea level (GMSL) projections are relative to the 1995–2014 baseline period (Kopp, Garner, et al., 2023). We present GMSL projections under the low-emissions SSP1-2.6 and high-emissions SSP5-8.5 scenarios (O'Neill et al., 2016).

The ice sheet and glacier components differ across the alternative IPCC AR6 projections. These alternative projections are referred to as “workflows” (Kopp, Garner, et al., 2023). We use workflows 1e, 2e, 3e, and 4 (Kopp, Garner, et al., 2023). Workflow 1e uses Antarctic ice sheet, Greenland ice sheet, and glacier components from a statistical emulator (Edwards et al., 2021; Fox-Kemper et al., 2021) of the multi-model ensembles of the Ice Sheet Model Intercomparison Project for CMIP6 (ISMIP6; S. Nowicki et al., 2020; S. M. J. Nowicki et al., 2016) and the Glacier Model Intercomparison Project (GlacierMIP; Marzeion et al., 2020). Workflow 2e uses different Antarctic ice sheet components, also based on statistical emulation of a multi-model ensemble (Levermann et al., 2020). Workflow 3e uses different Antarctic ice sheet components, based on results from a

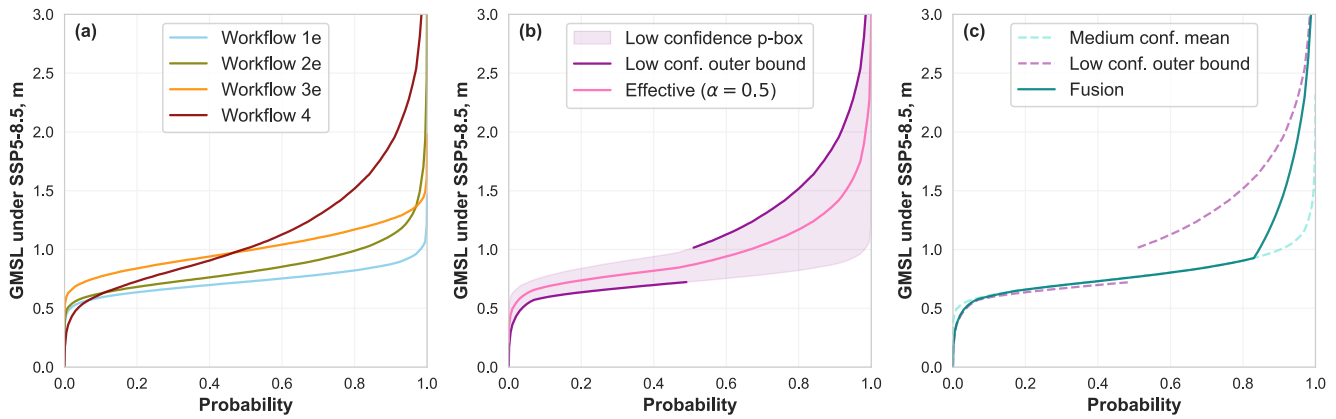


Figure 2. Quantile functions of GMSL in 2100 under SSP5-8.5. (a) The four alternative IPCC AR6 workflows. (b) The *low confidence* p-box (which spans the four workflows), the *low confidence* outer bound, and the ambiguity-neutral effective distribution (with equal weighting between the lower and upper bounds of the p-box). (c) The *medium confidence* mean (the mean of workflows 1e and 2e), the *low confidence* outer bound, and the fusion (which combines these distributions using the weighting function shown in Figure 3).

single Antarctic ice sheet model (DeConto et al., 2021) that includes a representation of marine ice cliff instability (MICI; Pollard et al., 2015). Workflow 4 uses different Antarctic and Greenland ice sheet components, both derived from structured expert judgment (Bamber et al., 2019). The structured expert judgment approach differs from that of an expert survey (Horton et al., 2020), which is not used here.

AR6 distinguishes between better-understood *medium confidence* processes, which can be explored using multi-model ensembles such as ISMIP6, and poorly-understood *low confidence* processes, such as MICI (Fox-Kemper et al., 2021; Kopp, Oppenheimer, et al., 2023; Slangen et al., 2023). Workflows 1e and 2e are categorized as *medium confidence* projections; workflows 3e and 4 are categorized as *low confidence* projections (Fox-Kemper et al., 2021; Kopp, Garner, et al., 2023).

2.2. Existing Approaches: Quantile Functions, p-Box, Bounds, and Effective Distribution

We define each probability distribution as a quantile function. A quantile function maps probability to values. A quantile function is the inverse of a cumulative distribution function, which maps values to probability. Following the IPCC AR6 sea-level projections (G. G. Garner et al., 2021), we use non-parametric quantile functions, defined at the following probabilities: 0.00 to 1.00 with an interval of 0.01 (corresponding to each integer percentile) and also at 0.001, 0.005, 0.995, and 0.999 (corresponding to the 0.1st, 0.5th, 99.5th, and 99.9th percentiles).

A p-box (probability box) is an envelope that spans the range of multiple quantile functions (Kopp, Oppenheimer, et al., 2023; Le Cozannet et al., 2017). The range across the p-box indicates ambiguity (Kopp, Oppenheimer, et al., 2023), “what is unknown” (Rohmer et al., 2019). There is no upper limit on the number of quantile functions that can be used to construct a p-box. In this paper, we construct the p-box using four quantile functions that correspond to the workflows described above: workflows 1e, 2e, 3e, and 4 (Figure 2b). This approach corresponds to the *low confidence* p-box of AR6 (Fox-Kemper et al., 2021).

The p-box is bounded by two quantile functions: a lower bound and an upper bound (Le Cozannet et al., 2017). The lower bound (L) corresponds to the minimum of the four workflows at each probability level ($0 \leq p \leq 1$):

$$L(p) = \min\{W_1(p), W_2(p), W_3(p), W_4(p)\} \quad (1)$$

where W_1 , W_2 , W_3 , and W_4 refer to the quantile functions of workflows 1e, 2e, 3e, and 4. Similarly, the upper bound (U) corresponds to the maximum of the four workflows:

$$U(p) = \max\{W_1(p), W_2(p), W_3(p), W_4(p)\} \quad (2)$$

Following the IPCC AR6 sea-level projections, we derive a *low confidence* outer bound (B) using the upper bound for probabilities above the median and the lower bound for probabilities below the median:

$$B(p) = \begin{cases} U(p), & 0.5 < p \leq 1 \\ \text{undefined}, & p = 0.5 \\ L(p), & 0 \leq p < 0.5 \end{cases} \quad (3)$$

At the median ($p = 0.5$), we adopt a convention that the median is undefined. This differs from the convention followed by the IPCC AR6 projections, where the median is defined as the mean of the medians across the workflows (G. G. Garner et al., 2021). Either way, the outer bound is not continuous across the median (Figure 2b). This discontinuity informs our decision to specify the median as undefined.

The effective distribution (E_a) is a weighted mean of the upper and lower bounds:

$$E_a(p) = a \cdot U(p) + (1 - a) \cdot L(p) \quad (4)$$

where the constant weight a ($0 \leq a \leq 1$) corresponds to a decision-maker's degree of ambiguity aversion (Dubois & Guyonnet, 2011; Rohmer et al., 2019). The choice of weight a is subjective (Dubois & Guyonnet, 2011). Here, we aim to provide an ambiguity-neutral estimate of the scientific uncertainty. Therefore, we show results for $a = 0.5$ (Rohmer et al., 2019): the ambiguity-neutral effective distribution ($E_{0.5}$) is the mean of the lower and upper bounds (Figure 2b). However, even this 'neutral' choice is subjective and may not align with the ambiguity aversion of a downstream decision-maker.

2.3. Fusion

We aim to provide a best estimate of the scientific uncertainty by considering the complementary strengths of the alternative workflows. Our proposed fusion is a quantile-dependent weighted-mean of other quantile functions. To identify these quantile functions, we ask two questions.

First, which quantile function do we assess to be most reliable in the center of the distribution? In other words, which quantile function provides the best estimate of the most-likely central possibilities? The two *medium confidence* workflows are strong candidates. Multi-model ensembles—such as ISMIP6—may skilfully represent many important ice sheet processes, enabling these ensembles to explore the uncertainty associated with these *medium confidence* processes (Goelzer et al., 2020; Payne et al., 2021). We therefore assume that the *medium confidence* workflows reliably sample the most-likely central possibilities, an assumption consistent with AR6 (Fox-Kemper et al., 2021). We have no preference between the two *medium confidence* workflows. Therefore, instead of selecting a single workflow, we choose to use the *medium confidence* mean (M), the mean of the quantile functions of workflows 1e and 2e:

$$M(p) = \frac{W_1(p) + W_2(p)}{2} \quad (5)$$

Second, which quantile function do we assess to be most reliable in the tails of the distribution? In other words, which quantile function provides the best estimate of the unlikely tail possibilities? The *low confidence* outer bound (B) is the strongest candidate. The outer bound incorporates uncertainty from all four workflows, including the *low confidence* workflows that account for poorly-understood ice sheet processes that increase the scientific uncertainty. In contrast, the *medium confidence* workflows may underestimate the full range of scientific uncertainty (Aschwanden et al., 2021).

Having answered these questions, we use a weighting function (w) to construct the fusion (F) using the quantile functions of the *medium confidence* mean (M) and the *low confidence* outer bound (B):

$$F(p) = w(p) \cdot M(p) + (1 - w(p)) \cdot B(p) \quad (6)$$

We now ask, what function should we choose for the weighting function (w)? Considering our assumptions, we seek a quantile-dependent weighting function that prioritizes the *medium confidence* mean in the center of the distribution and *low confidence* outer bound in the tails. A simple option would be to use a triangular weighting

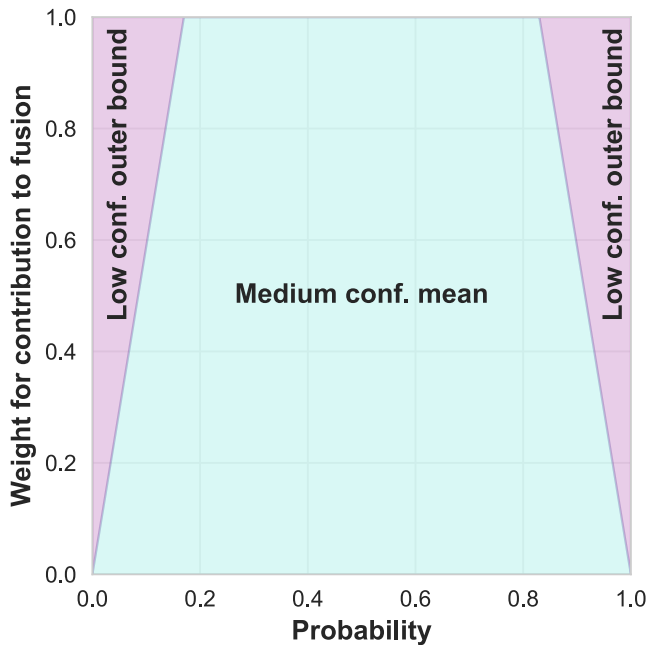


Figure 3. The trapezoidal weighting function (Equation 7) that combines the quantile functions of the *medium confidence* mean and the *low confidence* outer bound to produce the fusion (Equation 6).

function. However, to maintain consistency with the *likely* range of AR6 (Fox-Kemper et al., 2021; Kopp, Oppenheimer, et al., 2023), we use a trapezoidal weighting function (Figure 3):

$$w(p) = \begin{cases} \frac{1-p}{0.17}, & 0.83 < p \leq 1 \\ 1, & 0.17 \leq p \leq 0.83 \\ \frac{p}{0.17}, & 0 \leq p < 0.17 \end{cases} \quad (7)$$

In other words, the fusion follows the *medium confidence* mean between the 17th and 83rd percentiles and transitions smoothly to the *low confidence* outer bound in the tails. This is approximately consistent with the *likely* range of AR6, which was derived from the *medium confidence* outer bound (not the *medium confidence* mean). By assigning all the weight to the *medium confidence* mean in the center of the distribution, we avoid the discontinuity in the outer bound. This ensures that the fusion is continuous (Figure 2c). We also note that the *medium confidence* mean is contained within the p-box from which the outer bound is constructed. This ensures that the fusion is monotonic.

The fusion differs from a mixture distribution consisting of a weighted-mean of cumulative distribution functions. We have chosen to mix the quantile functions instead, because a quantile-dependent weighted-mean of quantile functions more accurately reflects our assumptions about the complementary strengths of the *medium confidence* and *low confidence* workflows.

3. Results

3.1. Alternative Workflows, p-Box, and Outer Bound

Model ambiguity drives uncertainty *within* each workflow (Figure 2a). For example, the ice sheet components of workflow 1e are derived from an ensemble of multiple ice sheet models. We do not know which model provides the most accurate description of real ice sheet behavior. By sampling multiple models through subjective averaging, workflow 1e effectively treats the multi-model ensemble as a proxy for scientific uncertainty.

Method ambiguity drives difference *between* workflows (Figure 2a). For example, *medium confidence* model-based and *low confidence* expert-based projections of ice sheet mass loss differ markedly, driving differences between workflows 1e and 4: workflow 4 has a higher median and covers a much wider uncertainty range. The *low confidence* p-box quantifies the method ambiguity (Figure 2b).

The *low confidence* outer bound is discontinuous at the median (Figure 2b). The discontinuity corresponds to a gap in the probability density function (Figure 4). Due to the discontinuity, the outer bound is not a well-behaved probability distribution.

3.2. Fusion

To provide a best estimate of the scientific uncertainty, the fusion combines information from the *medium confidence* and *low confidence* workflows. The fusion follows the *medium confidence* mean in the center of the distribution, whilst simultaneously incorporating the thick upper tail of the *low confidence* outer bound (Figures 2c and 4).

The fusion differs from the outer bound and the effective distribution. In contrast to the outer bound, the fusion is a well-behaved probability distribution, with no discontinuity at the median (Figure 2c). In contrast to the ambiguity-neutral effective distribution, the fusion has a lower median yet also has thicker tails, because it incorporates the full uncertainty range of the outer bound (Fig. S1 in Supporting Information S1).

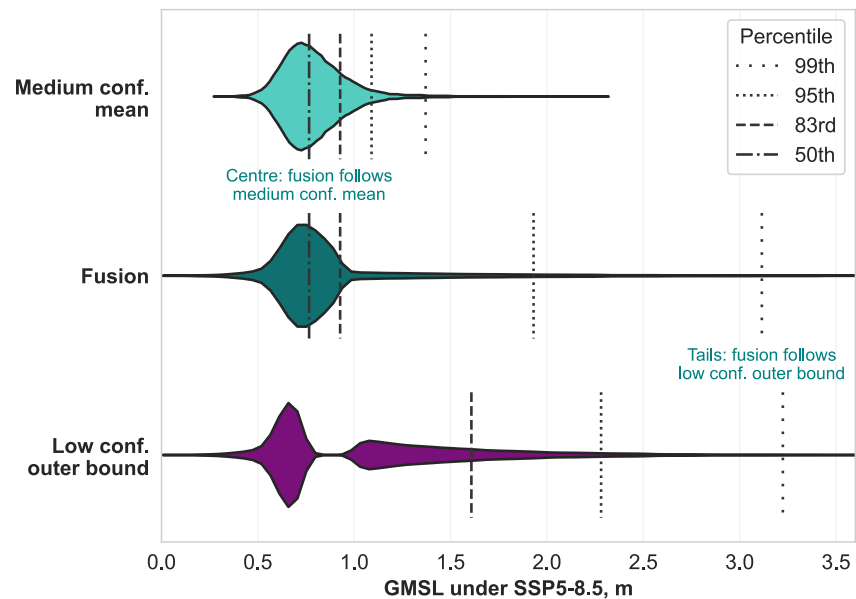


Figure 4. Probability density functions of GMSL in 2100 under SSP5-8.5. Each probability density function is derived from the corresponding quantile function using Monte Carlo sampling (with 1 million random samples drawn from a uniform distribution of probabilities) and is plotted as a kernel density estimate (using Scott's rule for bandwidth selection and limiting the range to that of the samples). The median, 83rd, 95th, and 99th percentiles are indicated by vertical lines. The median of the *low confidence* outer bound is undefined.

As a probabilistic projection, the fusion provides probabilistic answers. For example, the probability of GMSL exceeding 1.0 m by 2100 is 4% under the low-emissions SSP1-2.6 scenario (Figure 5). Under the high-emissions SSP5-8.5 scenario, the probability increases substantially to 16%. These precise probabilities summarize our best estimate of the scientific uncertainty. In contrast, the lower and upper bounds of the p-box quantify method ambiguity: across the four alternative workflows, the probability of GMSL exceeding 1.0 m ranges from 0% to 7% under SSP1-2.6 and from 2% to 51% under SSP5-8.5 (Figure 5).

3.3. Median, Likely Range, Very Likely Range, and High-End Projection

The fusion provides a median projection (50th percentile), *likely* range (17th–83rd percentiles), *very likely* range (5th–95th percentiles), and high-end projection (95th percentile) that are consistent with our assumptions about the complementary strengths of the alternative workflows. For GMSL in 2100 under SSP1-2.6, the median is 0.4 m, the *likely* range is 0.3–0.6 m, and the *very likely* range is 0.3–1.0 m (Figure 6a; Table 1). Under SSP5-8.5, the median is 0.8 m, the *likely* range is 0.6–0.9 m, and the *very likely* range is 0.5–1.9 m (Figure 6b; Table 1). For both scenarios, the *likely* range and median follow the *medium confidence* mean (Fig. S2 in Supporting Information S1). The *very likely* range falls between the 5th–95th percentile ranges of the *medium confidence* mean and the *low confidence* outer bound (Fig. S2 in Supporting Information S1).

A high-end projection can be derived from the upper end of the *very likely* range (95th percentile). For GMSL in 2100 under SSP5-8.5, this high-end projection is 1.9 m. This falls between the 83rd and 95th percentiles of the *low confidence* outer bound (1.6 and 2.3 m; Fig. S2 in Supporting Information S1).

4. Discussion

4.1. A Best Estimate of Scientific Uncertainty

The fusion provides an informed best estimate of scientific uncertainty, described probabilistically. To provide this best estimate, we have made transparent assumptions about the complementary strengths of existing projection workflows.

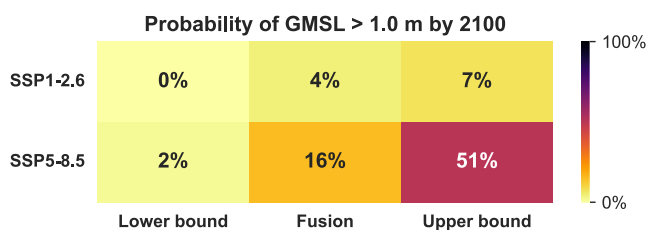


Figure 5. Probability of GMSL exceeding 1.0 m by 2100. Results are shown for the fusion, the lower bound of the *low confidence* p-box, and the upper bound, under both SSP1-2.6 and SSP5-8.5.

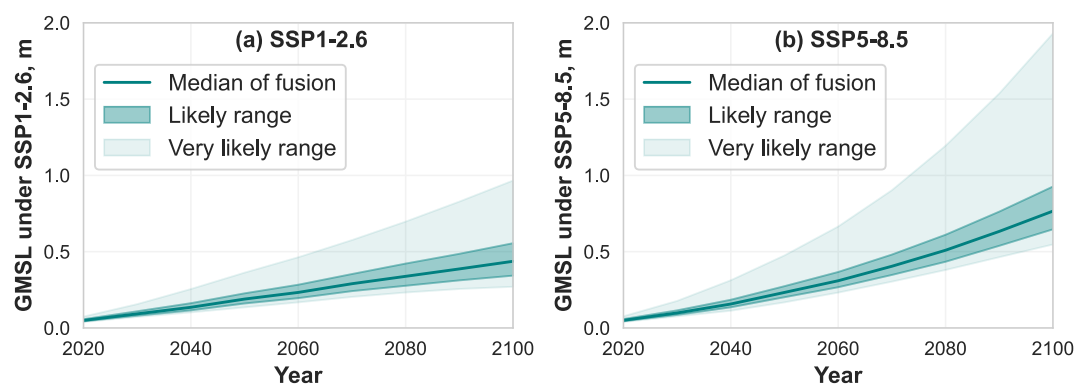


Figure 6. Median, *likely* range, and *very likely* range of GMSL, derived from the fusion under two emissions scenarios: (a) SSP1-2.6; (b) SSP5-8.5.

The fusion integrates information from models and experts. Expert judgment is necessary and valuable, informing model building, model evaluation, and the quantification of scientific uncertainty (Majszak & Jebeile, 2023). Climate scientists are the experts who are most qualified to characterize, assess, and convey the scientific uncertainty associated with climate change (Fischhoff & Davis, 2014). Accordingly, expert judgment is integral throughout the process of producing probabilistic projections (Figure 1; Majszak & Jebeile, 2023). We have proposed an additional layer of expert judgment in which experts consider the complementary strengths of alternative projections and identify a corresponding weighting function to produce the fusion. This additional layer of expert judgment could be provided by assessment panels, such as the IPCC. We anticipate, however, that consensus may pose a major challenge: Can the panel reach consensus on assumptions about the strengths of alternative projections and the corresponding weighting function to use? For example, experts may disagree about which projections to use for the most-likely central possibilities. One possible solution would be to use a weighted mean of alternative *medium confidence* workflows, with the weights determined by the votes of different experts.

The fusion is consistent with a Bayesian interpretation of probability. A probabilistic projection describes scientific uncertainty (Millner et al., 2013), a type of epistemic uncertainty (Dubois & Guyonnet, 2011; Hinkel et al., 2021; Shepherd, 2019): we possess only incomplete and imprecise knowledge of the physical climate system. A probabilistic projection must therefore be interpreted from a Bayesian (or “subjective”) perspective: the probability distribution represents “degrees of belief” about possible future outcomes (Hájek, 2019). These degrees of belief are conditioned on the assumptions and methods used to construct the probabilistic projection. Although a probabilistic projection may misrepresent the uncertainty when misinterpreted (Katzav et al., 2021), we would argue that probabilistic projections remain both justifiable and useful. Although a probability distribution derived from climate models may be distorted, this does not mean that we should abandon a probabilistic approach—idealized models can still provide valuable information about the real world (Dethier, 2023).

The fusion represents model ambiguity and method ambiguity consistently. Both model ambiguity and method ambiguity are represented probabilistically. This contrasts with the approach adopted in AR6 (Fox-Kemper et al., 2021), where model ambiguity was represented probabilistically within each workflow while method ambiguity was represented using p-boxes.

Table 1
Comparison of Published Projections of GMSL in 2100

Source	GMSL in 2100 under SSP1-2.6, m			GMSL in 2100 under SSP5-8.5, m			
	Median	Likely range	Very likely range	Median	Likely range	Very likely range	High-end projection
Fusion	0.4	0.3–0.6	0.3–1.0	0.8	0.6–0.9	0.5–1.9	1.9
IPCC AR6 <i>medium confidence</i> (Fox-Kemper et al., 2021)	0.4	0.3–0.6		0.8	0.6–1.0		
IPCC AR6 <i>low confidence</i> (Fox-Kemper et al., 2021)				0.9	0.6–1.6		1.6 (83rd percentile) 2.3 (95th percentile)
van de Wal et al. (2022)							1.6

The fusion complements and builds on the p-box approach. A p-box excels at emphasizing ambiguity. The existence of both a *medium confidence* p-box and a *low confidence* p-box in AR6 communicates an additional layer of ambiguity. However, the substantial ambiguity communicated by the p-boxes may hinder decision-making (Rohmer et al., 2019). Furthermore, although the p-box is not a probabilistic projection, there is a danger that users may misinterpret the outer bound as a precise probabilistic projection (cf. van der Pol & Hinkel, 2019). Additionally, the discontinuity in the outer bound can influence downstream results, such as the projected timing of decreased coastal protection (Hermans et al., 2023). In contrast to the outer bound, the fusion is a probabilistic projection and is continuous. We propose that climate scientists consider using both the p-box and the fusion: the p-box quantifies method ambiguity, while the fusion quantifies a best estimate of scientific uncertainty, conditioned on the scientists' assumptions.

The fusion complements and supports a storyline approach. A physically self-consistent storyline (Shepherd, 2019; Shepherd et al., 2018) can be referenced to a specific percentile of a probabilistic projection (Palmer et al., 2024). For example, we could develop a high-end sea-level storyline based on the 95th percentile of the fusion under SSP5-8.5.

4.2. Comparison With Other Projections

Importantly, the fusion provides a meaningful median (50th percentile), *likely* range (17th–83rd percentiles), *very likely* range (5th–95th percentiles), and high-end projection (95th percentile). Although any probabilistic projection can provide percentile ranges, the ranges are only meaningful if we trust the general reliability of the projection at those percentiles. Scientists must therefore consider their degree of trust in the underlying methods and assumptions, including our assumptions about the complementary strengths of the alternative workflows. If the fusion provides an informed best estimate of scientific uncertainty in both the center and the tails of the distribution, then the fusion provides a meaningful median, *likely* range, *very likely* range, and high-end projection.

These ranges can be interpreted as credible intervals. This differs slightly from the “imprecise” *likely* range of AR6, which was derived from the *medium confidence* outer bound (Fox-Kemper et al., 2021; Kopp, Oppenheimer, et al., 2023). Nevertheless, the fusion's median and *likely* range are very similar to those of the IPCC AR6 *medium confidence* projections (Table 1). In contrast, the *very likely* range is novel. By providing a meaningful *very likely* range, the fusion addresses the absence of a *very likely* range in AR6 (Fox-Kemper et al., 2021, p. 1298).

Under SSP5-8.5, the fusion's high-end projection is 1.9 m in 2100 (Table 1). This falls between the IPCC AR6's high-end projections of 1.6 and 2.3 m, which were derived from the 83rd and 95th percentiles of the *low confidence* outer bound. The fusion's high-end projection of 1.9 m is a little higher than van de Wal et al. (2022)'s high-end projection of 1.6 m, which was based on expert judgment of available evidence. In general, published high-end projections vary widely: A. J. Garner et al. (2018) reported that the range of published “upper projections” has expanded to 0.5–2.5 m since 2013. The fusion's high-end projection falls well within this range.

4.3. Meeting the Needs of Diverse Users

The fusion caters to diverse users with differing levels of uncertainty tolerance (Blankespoor et al., 2023; Hinkel et al., 2019). The assessment of scientific uncertainty is entrusted to sea-level scientists who can make informed choices about the complementary strengths of alternative projections. The downstream user only needs to choose which percentiles to use, supporting usability. Even though coastal practitioners may consider only a small number of decision-oriented scenarios (A. J. Garner et al., 2023; Hirschfeld et al., 2023), such scenarios can be derived from the fusion by selecting specific percentiles (Kopp, Oppenheimer, et al., 2023). For example, the 95th percentile is useful when planning activities with low uncertainty tolerance (New Jersey Department of Environmental Protection, 2021). The fusion also caters to users who require a full probability distribution of scientific uncertainty (Fischhoff & Davis, 2014; Rasmussen et al., 2020). For example, the fusion could facilitate more accurate estimation of coastal adaptation costs (Wong et al., 2022).

However, users must remember that sea-level projections remain subject to ambiguity (Kopp, Oppenheimer, et al., 2023). To quantify the influence of the method ambiguity, users can conduct sensitivity tests using the lower and upper bounds of the p-box. Alternatively, users may choose to adopt a “multiple priors” approach

(Hansen, 2014; Heal & Millner, 2014), treating the fusion as a “benchmark” projection (Text S1 in Supporting Information S1; Hansen, 2014). To communicate method ambiguity, we recommend that assessment panels publish either the p-box or individual workflows alongside the fusion.

Users must also remember that the fusion describes scientific uncertainty. The fusion does not describe other policy-relevant categories of uncertainty (Millner et al., 2013). The fusion does not incorporate decision-makers' values (Fischhoff & Davis, 2014). The fusion does not circumvent the need for local contextualization of sea-level assessments (Blankespoor et al., 2023). Beyond assessment, other aspects of the coastal adaptation cycle—planning, implementation, and monitoring—are essential and require further research (Cabana et al., 2023). Diverse disciplinary experts, practitioners, and local stakeholders offer complementary perspectives that can enrich sea-level science, enabling usability (Durand et al., 2022; Kopp et al., 2019).

5. Conclusions

Sea-level projections must cater to users with diverse needs and differing tolerance for uncertainty. Although many users may choose to use a single estimate of sea-level rise, the sea-level science community can simplify the choice by providing a single probabilistic projection from which users can select their preferred percentiles according to their uncertainty tolerance. We have proposed that this single probabilistic projection can be a fusion of alternative probabilistic projections. To produce the fusion, we have considered the complementary strengths of alternative projections. The fusion is an informed best estimate of scientific uncertainty, quantified using a probability distribution. Beyond quantification of uncertainty, the fusion also supports communication of uncertainty. The fusion caters to diverse users by providing meaningful information in both the center and the tails of the distribution.

The fusion will need to be updated periodically. We have demonstrated the fusion approach using the current generation of projections used by the IPCC (Fox-Kemper et al., 2021). As sea-level science, observations, and projections continue to evolve (A. J. Garner et al., 2018; Slangen et al., 2023), climate scientists will need to reconsider the strengths of alternative projections.

The fusion approach could be applied in various ways beyond those demonstrated here. We could produce a fusion using two or more alternative probabilistic projections of any variable. For example, we could produce a fusion that combines alternative probabilistic projections of Greenland ice sheet mass loss, vertical land movement, or global mean surface temperature. Most intriguingly, we could produce a fusion that combines alternative emissions scenarios. We intend to explore this topic further in future research.

Data Availability Statement

We downloaded the IPCC AR6 sea-level projections from <https://doi.org/10.5281/zenodo.6382554> (G. G. Garner et al., 2021). We have published our analysis and figure-production code at <https://doi.org/10.5281/zenodo.13627262> (Grandey, 2024).

References

- Aschwanden, A., Bartholomaeus, T. C., Brinkerhoff, D. J., & Truffer, M. (2021). Brief communication: A roadmap towards credible projections of ice sheet contribution to sea level. *The Cryosphere*, 15(12), 5705–5715. <https://doi.org/10.5194/tc-15-5705-2021>
- Bamber, J. L., Oppenheimer, M., Kopp, R. E., Aspinall, W. P., & Cooke, R. M. (2019). Ice sheet contributions to future sea-level rise from structured expert judgment. *Proceedings of the National Academy of Sciences*, 116(23), 11195–11200. <https://doi.org/10.1073/pnas.1817205116>
- Bamber, J. L., Oppenheimer, M., Kopp, R. E., Aspinall, W. P., & Cooke, R. M. (2022). Ice sheet and climate processes driving the uncertainty in projections of future sea level rise: Findings from a structured expert judgement approach. *Earth's Future*, 10(10). <https://doi.org/10.1029/2022EF002772>
- Blankespoor, B., Dasgupta, S., Wheeler, D., Jeuken, A., Van Ginkel, K., Hill, K., & Hirschfeld, D. (2023). Linking sea-level research with local planning and adaptation needs. *Nature Climate Change*, 13(8), 760–763. <https://doi.org/10.1038/s41558-023-01749-7>
- Cabana, D., Rölfer, L., Evadzi, P., & Celliers, L. (2023). Enabling climate change adaptation in coastal systems: A systematic literature review. *Earth's Future*, 11(8), e2023EF003713. <https://doi.org/10.1029/2023EF003713>
- DeConto, R. M., Pollard, D., Alley, R. B., Velicogna, I., Gasson, E., Gomez, N., et al. (2021). The Paris climate agreement and future sea-level rise from Antarctica. *Nature*, 593(7857), 83–89. <https://doi.org/10.1038/s41586-021-03427-0>
- Dethier, C. (2023). Against “possibilist” interpretations of climate models. *Philosophy of Science*, 90(5), 1–1426. <https://doi.org/10.1017/psa.2023.6>
- Dubois, D., & Guyonnet, D. (2011). Risk-informed decision-making in the presence of epistemic uncertainty. *International Journal of General Systems*, 40(2), 145–167. <https://doi.org/10.1080/03081079.2010.506179>

Acknowledgments

This Research/Project is supported by the National Research Foundation, Singapore, and National Environment Agency, Singapore under the National Sea Level Programme Funding Initiative (Award USS-IF-2020-3). BPH was also supported by Singapore Ministry of Education (MOE) Academic Research Fund Tier 3 Project MOE-2019-T3-1-004. We thank the projection authors for developing and making the sea level rise projections available, multiple funding agencies for supporting the development of the projections, and the NASA Sea Level Change Team for developing and hosting the IPCC AR6 Sea Level Projection Tool. BSG thanks Robert Kopp for providing helpful advice about the IPCC AR6 projections data. BSG thanks Dhruvajyoti Samanta, Jennifer Weeks, Trina Ng, Nidheesh Gangadharan, and Steven Sherwood for helpful discussions. This work comprises Earth Observatory of Singapore contribution number 629.

- Durand, G., Van Den Broeke, M. R., Le Cozannet, G., Edwards, T. L., Holland, P. R., Jourdain, N. C., et al. (2022). Sea-level rise: From global perspectives to local services. *Frontiers in Marine Science*, 8, 709595. <https://doi.org/10.3389/fmars.2021.709595>
- Edwards, T. L., Nowicki, S., Marzeion, B., Hock, R., Goelzer, H., Seroussi, H., et al. (2021). Projected land ice contributions to twenty-first-century sea level rise. *Nature*, 593(7857), 74–82. <https://doi.org/10.1038/s41586-021-03302-y>
- Ellsberg, D. (1961). Risk, ambiguity, and the savage axioms. *Quarterly Journal of Economics*, 75(4), 643. <https://doi.org/10.2307/1884324>
- Fischhoff, B., & Davis, A. L. (2014). Communicating scientific uncertainty. *Proceedings of the National Academy of Sciences*, 111(supplement_4), 13664–13671. <https://doi.org/10.1073/pnas.1317504111>
- Fox-Kemper, B., Hewitt, H. T., Xiao, C., Aðalgeirsdóttir, G., Drijfhout, S. S., Edwards, T. L., et al. (2021). Ocean, cryosphere and sea level change. In V. Masson-Delmotte, P. Zhai, A. Pirani, S. L. Connors, C. Péan, S. Berger, et al. (Eds.), *Climate change 2021: The physical science basis. Contribution of working Group I to the Sixth assessment Report of the Intergovernmental panel on climate change* (pp. 1211–1362). Cambridge University Press. <https://doi.org/10.1017/9781009157896.011>
- Garner, A. J., Sosa, S. E., Tan, F., Tan, C. W. J., Garner, G. G., & Horton, B. P. (2023). Evaluating knowledge gaps in sea-level rise assessments from the United States. *Earth's Future*, 11(2). <https://doi.org/10.1029/2022EF003187>
- Garner, A. J., Weiss, J. L., Parris, A., Kopp, R. E., Horton, R. M., Overpeck, J. T., & Horton, B. P. (2018). Evolution of 21st century sea level rise projections. *Earth's Future*, 6(11), 1603–1615. <https://doi.org/10.1029/2018EF000991>
- Garner, G. G., Hermans, T., Kopp, R. E., Slangen, A. B., Edwards, A., Levermann, A., et al. (2021). IPCC AR6 sea level projections (version 20210809) [Dataset]. *Zenodo*. <https://doi.org/10.5281/zenodo.6382554>
- Goelzer, H., Nowicki, S., Payne, A., Larour, E., Seroussi, H., Lipscomb, W. H., et al. (2020). The future sea-level contribution of the Greenland ice sheet: A multi-model ensemble study of ISMIP6. *The Cryosphere*, 14(9), 3071–3096. <https://doi.org/10.5194/tc-14-3071-2020>
- Grandey, B. S. (2024). Analysis code for fusion of probabilistic projections of sea-level rise (d23a-fusion) (Version v0.3.0). *Zenodo*. <https://doi.org/10.5281/zenodo.13627262>
- Hájek, A. (2019). Interpretations of probability. In E. N. Zalta (Ed.), *The Stanford Encyclopedia of Philosophy (fall 2019)*. Metaphysics Research Lab, Stanford University. Retrieved from <https://plato.stanford.edu/archives/fall2019/entries/probability-interpret/>
- Hansen, L. P. (2014). Nobel lecture: Uncertainty outside and inside economic models. *Journal of Political Economy*, 122(5), 945–987. <https://doi.org/10.1086/678456>
- Heal, G., & Millner, A. (2014). Reflections: Uncertainty and decision making in climate change economics. *Review of Environmental Economics and Policy*, 8(1), 120–137. <https://doi.org/10.1093/reep/ret023>
- Hermans, T. H. J., Malagón-Santos, V., Katsman, C. A., Jane, R. A., Rasmussen, D. J., Haasnoot, M., et al. (2023). The timing of decreasing coastal flood protection due to sea-level rise. *Nature Climate Change*, 13(4), 359–366. <https://doi.org/10.1038/s41558-023-01616-5>
- Hinkel, J., Church, J. A., Gregory, J. M., Lambert, E., Le Cozannet, G., Lowe, J., et al. (2019). Meeting user needs for sea level rise information: A decision analysis perspective. *Earth's Future*, 7(3), 320–337. <https://doi.org/10.1029/2018EF001071>
- Hinkel, J., Feyen, L., Hemer, M., Le Cozannet, G., Lincke, D., Marcos, M., et al. (2021). Uncertainty and bias in global to regional scale assessments of current and future coastal flood risk. *Earth's Future*, 9(7). <https://doi.org/10.1029/2020EF001882>
- Hirschfeld, D., Behar, D., Nicholls, R. J., Cahill, N., James, T., Horton, B. P., et al. (2023). Global survey shows planners use widely varying sea-level rise projections for coastal adaptation. *Communications Earth & Environment*, 4(1), 102. <https://doi.org/10.1038/s43247-023-00703-x>
- Horton, B. P., Khan, N. S., Cahill, N., Lee, J. S. H., Shaw, T. A., Garner, A. J., et al. (2020). Estimating global mean sea-level rise and its uncertainties by 2100 and 2300 from an expert survey. *Npj Climate and Atmospheric Science*, 3(1), 18. <https://doi.org/10.1038/s41612-020-0121-5>
- Horton, B. P., Kopp, R. E., Garner, A. J., Hay, C. C., Khan, N. S., Roy, K., & Shaw, T. A. (2018). Mapping sea-level change in time, space, and probability. *Annual Review of Environment and Resources*, 43(1), 481–521. <https://doi.org/10.1146/annurev-environ-102017-025826>
- Katzav, J., Thompson, E. L., Risbey, J., Stainforth, D. A., Bradley, S., & Frisch, M. (2021). On the appropriate and inappropriate uses of probability distributions in climate projections and some alternatives. *Climatic Change*, 169(1–2), 15. <https://doi.org/10.1007/s10584-021-03267-x>
- Kopp, R. E., Garner, G. G., Hermans, T. H. J., Jha, S., Kumar, P., Reedy, A., et al. (2023b). The framework for assessing changes to sea-level (FACTS) v1.0: A platform for characterizing parametric and structural uncertainty in future global, relative, and extreme sea-level change. *Geoscientific Model Development*, 16(24), 7461–7489. <https://doi.org/10.5194/gmd-16-7461-2023>
- Kopp, R. E., Gilmore, E. A., Little, C. M., Lorenzo-Trueba, J., Ramenzoni, V. C., & Sweet, W. V. (2019). Useable science for managing the risks of sea-level rise. *Earth's Future*, 7(12), 1235–1269. <https://doi.org/10.1029/2018EF001145>
- Kopp, R. E., Oppenheimer, M., O'Reilly, J. L., Drijfhout, S. S., Edwards, T. L., Fox-Kemper, B., et al. (2023a). Communicating future sea-level rise uncertainty and ambiguity to assessment users. *Nature Climate Change*, 13(7), 648–660. <https://doi.org/10.1038/s41558-023-01691-8>
- Le Cozannet, G., Manceau, J.-C., & Rohmer, J. (2017). Bounding probabilistic sea-level projections within the framework of the possibility theory. *Environmental Research Letters*, 12(1), 014012. <https://doi.org/10.1088/1748-9326/aa5528>
- Levermann, A., Winkelmann, R., Albrecht, T., Goelzer, H., Golledge, N. R., Greve, R., et al. (2020). Projecting Antarctica's contribution to future sea level rise from basal ice shelf melt using linear response functions of 16 ice sheet models (LARMIP-2). *Earth System Dynamics*, 11(1), 35–76. <https://doi.org/10.5194/esd-11-35-2020>
- Majszak, M., & Jebeile, J. (2023). Expert judgment in climate science: How it is used and how it can be justified. *Studies in History and Philosophy of Science*, 100, 32–38. <https://doi.org/10.1016/j.shpsa.2023.05.005>
- Marzeion, B., Hock, R., Anderson, B., Bliss, A., Champollion, N., Fujita, K., et al. (2020). Partitioning the uncertainty of ensemble projections of global glacier mass change. *Earth's Future*, 8(7). <https://doi.org/10.1029/2019EF001470>
- Millner, A., Dietz, S., & Heal, G. (2013). Scientific ambiguity and climate policy. *Environmental and Resource Economics*, 55(1), 21–46. <https://doi.org/10.1007/s10640-012-9612-0>
- New Jersey Department of Environmental Protection. (2021). Sea-level rise guidance of New Jersey. Retrieved from <https://www.nj.gov/dep/bcrp/resilientnj/docs/dep-guidance-on-sea-level-rise-2021.pdf>
- Nowicki, S., Goelzer, H., Seroussi, H., Payne, A. J., Lipscomb, W. H., Abe-Ouchi, A., et al. (2020). Experimental protocol for sea level projections from ISMIP6 stand-alone ice sheet models. *The Cryosphere*, 14(7), 2331–2368. <https://doi.org/10.5194/tc-14-2331-2020>
- Nowicki, S. M. J., Payne, A., Larour, E., Seroussi, H., Goelzer, H., Lipscomb, W., et al. (2016). Ice sheet model intercomparison project (ISMIP6) contribution to CMIP6. *Geoscientific Model Development*, 9(12), 4521–4545. <https://doi.org/10.5194/gmd-9-4521-2016>
- O'Neill, B. C., Tebaldi, C., Van Vuuren, D. P., Eyring, V., Friedlingstein, P., Hurtt, G., et al. (2016). The scenario model intercomparison project (ScenarioMIP) for CMIP6. *Geoscientific Model Development*, 9(9), 3461–3482. <https://doi.org/10.5194/gmd-9-3461-2016>
- Palmer, M. D., Harrison, B. J., Gregory, J. M., Hewitt, H. T., Lowe, J. A., & Weeks, J. H. (2024). A framework for physically consistent storylines of UK future mean sea level rise. *Climatic Change*, 177(7), 106. <https://doi.org/10.1007/s10584-024-03734-1>

- Payne, A. J., Nowicki, S., Abe-Ouchi, A., Agosta, C., Alexander, P., Albrecht, T., et al. (2021). Future sea level change under coupled model intercomparison project phase 5 and phase 6 scenarios from the Greenland and Antarctic Ice Sheets. *Geophysical Research Letters*, *48*(16). <https://doi.org/10.1029/2020GL091741>
- Pollard, D., DeConto, R. M., & Alley, R. B. (2015). Potential Antarctic Ice Sheet retreat driven by hydrofracturing and ice cliff failure. *Earth and Planetary Science Letters*, *412*, 112–121. <https://doi.org/10.1016/j.epsl.2014.12.035>
- Rasmussen, D. J., Buchanan, M. K., Kopp, R. E., & Oppenheimer, M. (2020). A flood damage allowance framework for coastal protection with deep uncertainty in sea level rise. *Earth's Future*, *8*(3), e2019EF001340. <https://doi.org/10.1029/2019EF001340>
- Rodziewicz, D., Amante, C. J., Dice, J., & Wahl, E. (2022). Housing market impairment from future sea-level rise inundation. *Environment Systems and Decisions*, *42*(4), 637–656. <https://doi.org/10.1007/s10669-022-09842-6>
- Rohmer, J., Le Cozannet, G., & Manceau, J.-C. (2019). Addressing ambiguity in probabilistic assessments of future coastal flooding using possibility distributions. *Climatic Change*, *155*(1), 95–109. <https://doi.org/10.1007/s10584-019-02443-4>
- Shepherd, T. G. (2019). Storyline approach to the construction of regional climate change information. *Proceedings of the Royal Society A*, *475*(2225), 20190013. <https://doi.org/10.1098/rspa.2019.0013>
- Shepherd, T. G., Boyd, E., Calel, R. A., Chapman, S. C., Dessai, S., Dima-West, I. M., et al. (2018). Storylines: An alternative approach to representing uncertainty in physical aspects of climate change. *Climatic Change*, *151*(3–4), 555–571. <https://doi.org/10.1007/s10584-018-2317-9>
- Slangen, A. B. A., Palmer, M. D., Camargo, C. M. L., Church, J. A., Edwards, T. L., Hermans, T. H. J., et al. (2023). The evolution of 21st century sea-level projections from IPCC AR5 to AR6 and beyond. *Cambridge Prisms: Coastal Futures*, *1*, e7. <https://doi.org/10.1017/cft.2022.8>
- van der Pol, T. D., & Hinkel, J. (2019). Uncertainty representations of mean sea-level change: A telephone game? *Climatic Change*, *152*(3–4), 393–411. <https://doi.org/10.1007/s10584-018-2359-z>
- van de Wal, R. S. W., Nicholls, R. J., Behar, D., McInnes, K., Stammer, D., Lowe, J. A., et al. (2022). A high-end estimate of sea level rise for practitioners. *Earth's Future*, *10*(11). <https://doi.org/10.1029/2022EF002751>
- Wong, T. E., Ledna, C., Rennels, L., Sheets, H., Erickson, F. C., Diaz, D., & Anthoff, D. (2022). Sea level and socioeconomic uncertainty drives high-end coastal adaptation costs. *Earth's Future*, *10*(12), e2022EF003061. <https://doi.org/10.1029/2022EF003061>

References From the Supporting Information

- Hansen, L. P., & Marinacci, M. (2016). Ambiguity aversion and model misspecification: An economic perspective. *Statistical Science*, *31*(4). <https://doi.org/10.1214/16-STSS70>